Original Paper (Invited)

Krzysztof Jóźwik[*a], Adam Papierski[a], Krzysztof Sobczak[a], Damian Obidowski[a], Władysław Kryłłowicz[a], Emil Marciniak[b], Grzegorz Wróbel[c], Adrian Marciniak[d], Piotr Wróblewski[d], Agnieszka Kobierska[d], Łukasz Frączczak[d], Leszek Podsędkowski[d]

Radial fan controlled with impeller movable blades – CFD investigations

[a] Institute of Turbomachinery, Lodz University of Technology, 219/223 Wólczańska, 90-924 Łódź, Poland

[b] PhD student at the Institute of Turbomachinery, Lodz University of Technology, 219/223 Wólczańska, 90-924 Łódź, Poland

[c] Vibroson Lodz Limited, 10 Wileńska, 94-029 Łódź, Poland

[d] Institute of Machine Tools and Production Engineering, Lodz University of Technology, 1/15 Stefanowskiego, 90-924 Łódź, Poland

Abstract

Modern classical power generation systems, based on power plants in Poland, where coal (hard bituminous coal or lignite) is the primary energy source, operate under variable loading conditions. Thus, all machines working in the technological system of the power generation unit are required to be adapted to variable loading, and, consequently, to operate beyond the design point of their performance characteristics. High efficiency of the process requires the efficiency of individual devices to be high, beyond the design point, as well. For both air and exhaust gases fans, an effective control system is needed to attain a high level of efficiency. As a result of cooperation between two institutes from the Faculty of Mechanical Engineering, Lodz University of Technology, and the Vibroson company, a new design of the radial fan with impeller movable blades, which allows for controlling the device operation within a wide range, has been developed. This new design and determination the performance characteristics for two geometrical variants of blades with computational fluid dynamics methods are presented. The obtained results have been compared to the results of the measurements of fan performance curves conducted on the test stand.

Keywords: Radial fan control systems; CFD methods; Radial fan performance; Partial load

*Corresponding Author. Email address: krzysztof.jozwik@p.lodz.pl

Nomenclature

BC	–	boundary conditions
F	–	force, N
$\dot{m}$	–	mass flow rate, kg/s
M_o	–	torque, Nm
Q	–	volume flow rate, m^3/s
Q_n	–	nominal volume flow rate or volume flow rate at the rated point, m^3/s
P	–	power, W
P_b	–	loss of power (fanning loss), W
Δp_c	–	total compression ratio, Pa
η	–	efficiency
ρ	–	density, kg/m^3

1   Introduction

The designing process of any arbitrary technical object most often involves the determination of its parameters and geometry for the so-called design point (also referred to as the nominal point). However, in numerous instances these objects operate under conditions that are different from those defined during the designing process. It is important that the efficiency of such objects should be also as high as possible under these circumstances.

The efficiency of a power generation unit depends not only on the efficiency of conversion of the energy included in the fuel during the transformation into the electrical energy, but the efficiency of all devices whose operation is indispensable for technological processes involved in energy generation. Among such devices, one can mention fans. Their task is to provide fresh air to the combustion process (primary and secondary air), and to remove exhaust gases as well. Measurements of the fan operation capability were conducted many times and their efficiency calculated for a longer operation life (for instance, one year) does not exceed 50%. This refers both to the devices being already in operation and these newly designed. For the latter ones, designers foresee a certain margin of operating parameters covering unpredictable situations during the boiler operation (e.g., coal characterized by a low calorific value) [1–4].

The fan operation beyond the conditions for the design point is possible when a proper control system is applied. In general, the issue of fan control can concern:

- maintenance of constant pressure at the outlet for variable fan output,
- maintenance of constant fan output at variable operating conditions – variable resistance of the network.

Nowadays, control methods can be carried out by means of one of the following ways:

- change in the rotational speed of the motor that drives the fan,
- change in impeller blading angles in fans,
- application of guide vanes and alternations in guide vanes settings,
- throttling of the medium at suction,
- throttling of the medium at pumping,
- breakout of the medium into the atmosphere or recirculation of the medium surplus to the suction pipe [5,6].

Control via changes in angles of the impeller blading has not been used in radial fans so far. The investigations on this type of control systems have been conducted but due to some technical difficulties in introducing alternations in impeller blade angles or blade parts, this system has not been implemented in industrial applications yet [7,8].

If the above-mentioned control systems are considered, the modernization process has additionally to account for design limitations resulting from the state of the existing infrastructure at the site. Thus, significant exclusions of particular control systems can occur due to a physical lack of room to assemble them [3,4].

2 Object and its modifications

A new control system was assembled during modernization of the secondary air fan in the boiler no. 3 installation in Turów Power Plant. The fan under consideration is a single-suction radial device. The nominal fan output was equal to 68 m^3/s, and, in practice, at the full boiler output, it delivered only 54 m^3/s, that is to say, less than 80% of the nominal output. Such a deficiency (actually impossible to be used due too low motor output) caused very low fan efficiency, both under the full boiler output – 66%, as well as at its low loading – 37%. It should be underlined that the power generation unit operates nearly half its time at the minimal power – 120 MW. Such low efficiency was a source of very significant energy losses, followed by lowering the effective power of the unit as well, an increase in emissions of CO_2 and other components of exhaust gases that are hazardous to the natural environment. Low, if compared to the nominal one, efficiency of the fan caused that its operation was unsteady. It resulted in air flow pulsations that were followed by very high vibrations of the casing and suction pipes. Despite repairs and stiffeners that were introduced, cracks resulting in breaks in the unit operation often occurred. They contributed to a much lower functionality of the power generation unit.

The fan design, the unmated drive, as well as the operating conditions and requirements following from the actual loading were direct causes of a decision to

modernize the device. The structural limitations resulting from the installation arrangement allowed for an application of almost any arbitrary system of control.

For the fan under consideration, a solution that includes a control system based on fan impeller movable blades was proposed (Fig. 1). The impeller of the proposed design consists of a load-carrying disk, a fixed part of the impeller blade, a moveable part of the blade with an axis of rotation placed in the gravity center of this part of the blade, and a covering disk. The length of the blade movable part is equal to half the length of the fixed blade.
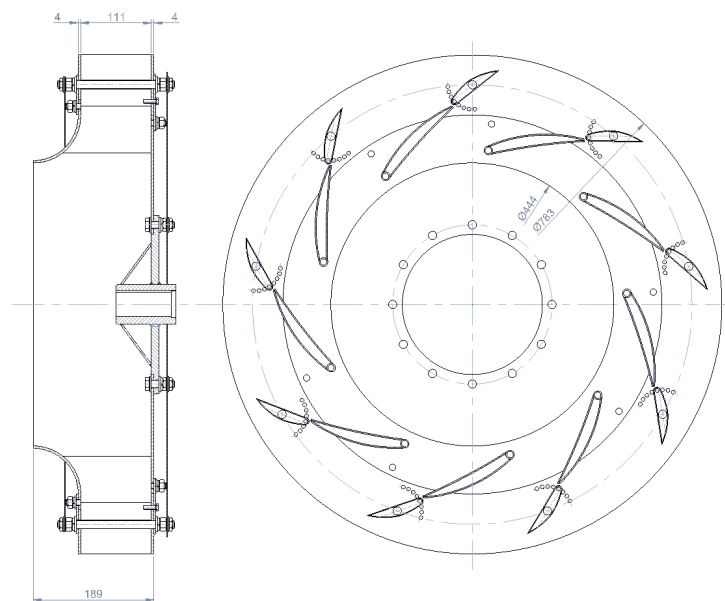
Figure 1: Modified impeller of the radial fan – technical drawing.

A general view of the newly designed structure is shown in Fig. 2. The fan inlet diameter is 444 mm. The impeller inner diameter is equal to 784 mm, and its width along the outer diameter equals 111 mm. The volute outlet channel is rectangular and has the following dimensions in its cross-section: 600 mm×300 mm.

The impeller blade tips can alter their angular position with respect to the fixed part of the blade. Two versions of movable parts of blades were made. They differed in the shape of their tips (cut or sharp). Some selected positions of the blade movable part and tip shapes are shown in Fig. 3.

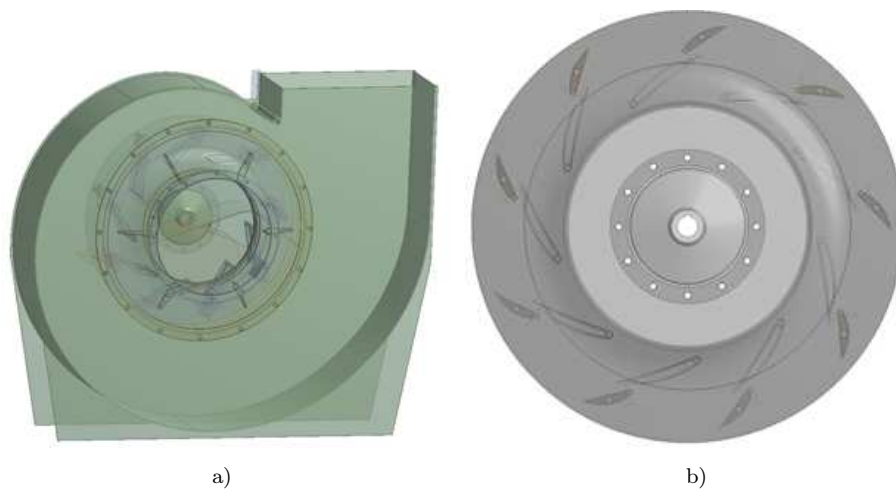a)   b)

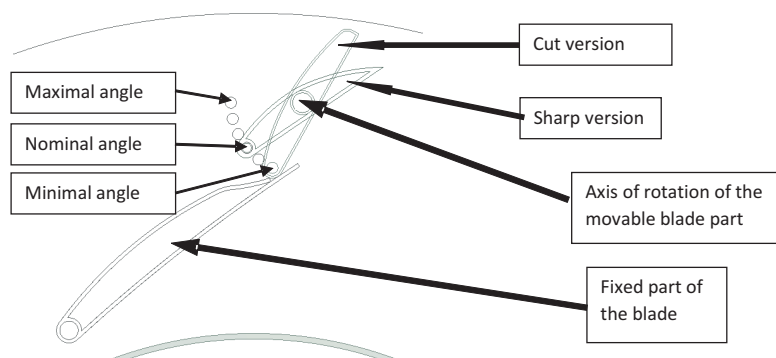Figure 2: Modified radial fan: a) general view, b) impeller with movable blade tips [9].

Figure 3: Shape and versions of the radial fan blade with a movable blade part.

For the impeller designed in this way, a flow numerical analysis and experimental investigations on a test stand were carried out. Both the numerical analysis and the experimental tests were aimed at determination of the performance characteristics of the fan for the nominal working point and the points determined by extreme positions of the movable part of the impeller blade, which is equivalent to the fan operation characterized by lower efficiency. The performance characteristics were determined for both the proposed versions of movable impeller blade tips. Finally, a comparison of the obtained calculated and experimentally determined performance characteristics was made.

3   Computational fluid dynamics investigations

The numerical analysis of the flow in the radial fan was aimed at determination of the flow and performance characteristics. To achieve this, an analysis of geometrical variants should be conducted, proper boundary conditions that have to correspond to the conditions during the experimental investigations should be defined, initial conditions for computations should be imposed, and, first of all, meshes of finite elements, which ought to be evaluated as far as their independency, i.e., a lack of the effect of mesh parameters on computational results within the assumed tolerance of alternations in the values of parameters assumed as essential, is concerned, should be generated. The numerical analysis was carried out for three angular positions of the movable impeller blade part and for two versions of its tips.

3.1   Meshes

For each version of the blade position and their tip geometry, meshes were generated. The differences referred to impeller meshes, in the part concerning the so-called palisade domain in particular. An example of the impeller mesh is depicted in Fig. 4.
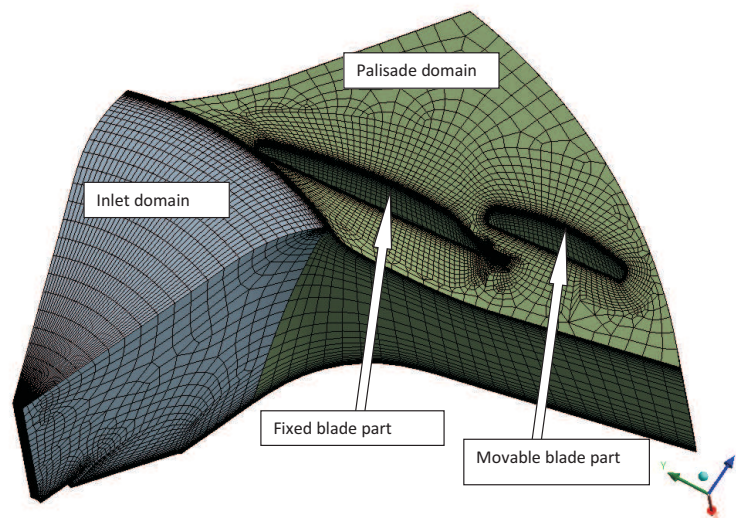

Figure 4: General view of an impeller mesh for the selected single path channel [9].

A mesh for the impeller inlet domain was built of hexahedral elements with the 'sweep method' that consists in generation of a mesh on the surface, and then

its multiplication by a given number of times along the defined direction. In this case, a mesh on the surface periodicity was generated and then it was swept towards the second surface periodicity. The mesh of the palisade domain was also generated with the 'sweep method'. In this case, the mesh was swept from the impeller shroud surface towards the impeller hub surface. The 'O-type' mesh was used around the impeller blades, generating thus 21 inflation layers at maximum, with the first layer thickness equal to 0.1 mm. The layer thickness increment coefficient was 1.27.

Figure 5 presents a number of mesh elements and statistics of a single impeller channel for individual positions of the movable blade in its cut and sharp version.

To discretise the volute computational domains, the ICEM CFD software to generate structural meshes that can be highly interfered by the user in individual regions, which as a result allows for generation of high-quality meshes, was used [11]. An example of the computational mesh for the fan volute is shown in Fig. 6.

The mesh topology was based on the letter Q. In this case, the mesh was defined for the volute cross-section used then to generate a mesh of a similar distribution of nodes around the volute axis, and, next, a segment was isolated from the channel outlet to its inside, which was added to the volute mesh along its circumference. The mesh was densified in the neighborhood of walls, and the density of elements in the impeller outlet zone and the gap at the impeller inlet were adapted. The generated mesh is composed of 3.7 million nodes and 3.6 million elements. High quality parameters of the mesh were attained: the smallest angle of 34.8°, the highest value of the aspect ratio – 146, the lowest value of quality – 0.419, changes in the value of volume – 3.3. In the calculations, main screw connections rotating with the impeller were accounted for. To achieve this, spaces around the screw connections were cut off from the volute volume. The volute with some volumes cut off was discretized in the way close to the above described, whereas the volumes around the screws were divided into tetrahedral-prismatic elements in a separate step.

The cross-section of the mesh obtained for the volute used in the computations covering the screw connections on the impeller is illustrated in Fig. 7. The following mesh parameters were attained: 3.5 million of nodes and 3.3 million of elements, the smallest angle of 35.8°, the highest value of the aspect ratio – 147, the lowest value of quality – 0.515, change in the value of volume – 2.8. Due to repeatability of geometries, the mesh was prepared for the section 120°, and then during the preprocessing, it was copied and connected with the remaining parts with interfaces, correspondingly. To simplify the mesh generation, threads were

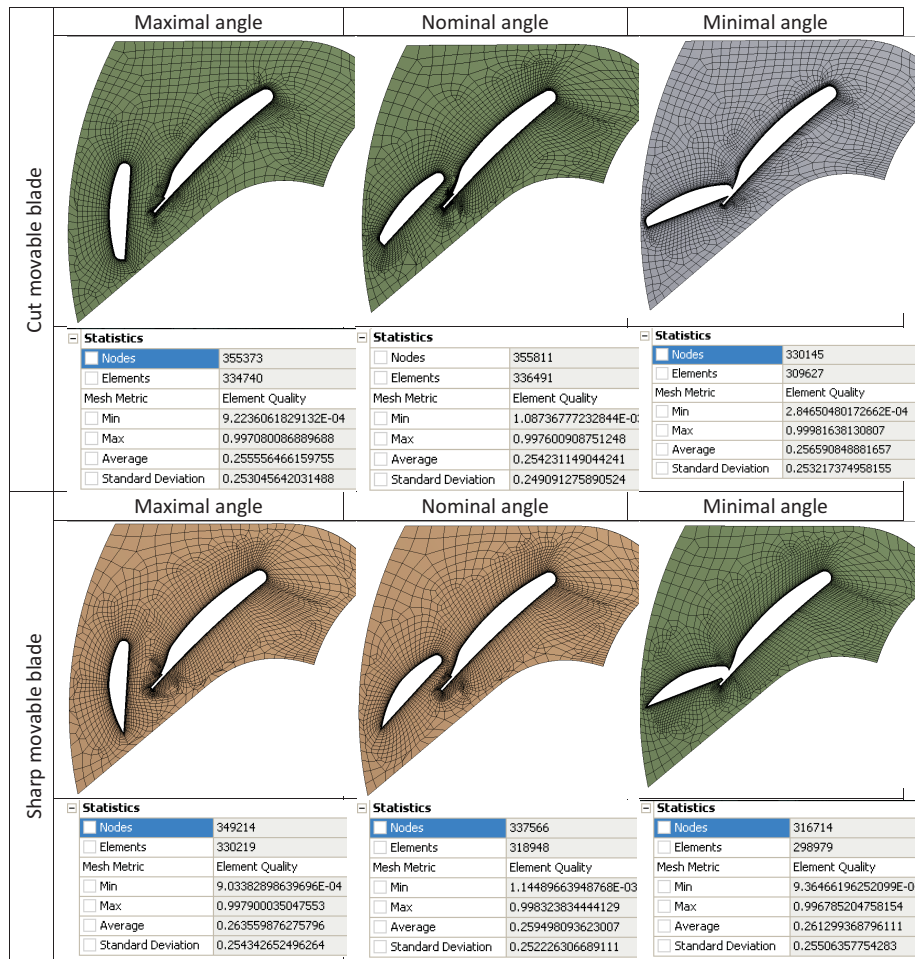|	Maximal angle	Nominal angle	Minimal angle

Figure 5: Impeller meshes and their statistics for all versions under investigation [9].

neglected on the screw surfaces and the washers were replaced with elongation of the hexagonal shape of the nuts up to the walls. A formation of the prismatic layer on surfaces of nuts and bolts was neglected as well.

Finally, a mesh of the following parameters: 784 thousand nodes and 3.8 million elements for the shroud zone, and 707 thousand nodes and 3.2 million elements for the hub zone was generated. The smallest angle was equal to 19.6° – shroud and 17.1° – hub, the highest value of aspect ratio – 32.5 and 30.6, correspond-
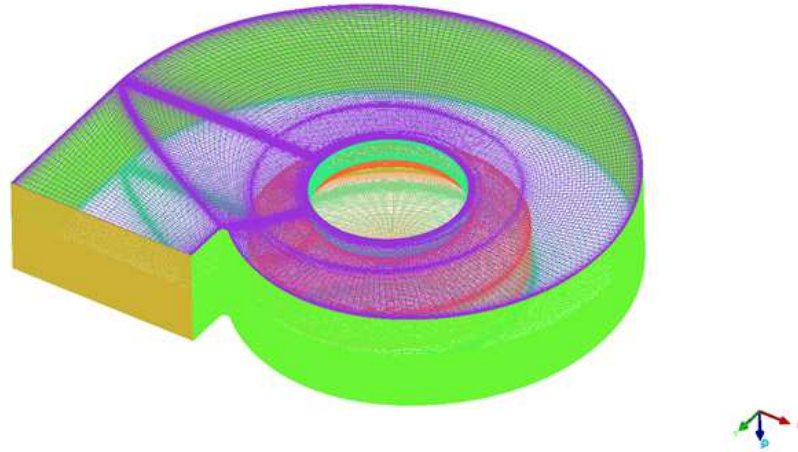
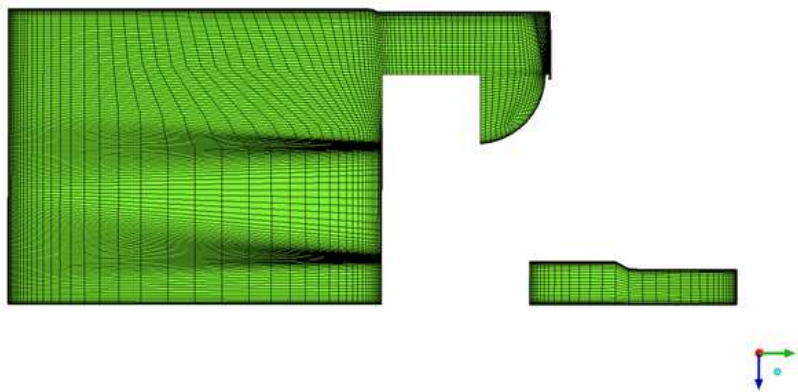Figure 6: General view of a mesh of the fan volute [9].

Figure 7: Distribution of volute mesh nodes in a cross-section – the mesh used in the calculations taking into account screws [9].

ingly, the lowest value of quality – 0.36 and 0.32, respectively, volume change – 16.0 (shroud) and 15.7(hub). Although, which is obvious, the mesh quality in these zones is significantly lower than that of the hexahedral mesh of the volute, it turned out to be sufficient to conduct steady flow calculations. Despite the fact that the mesh does not have zones around screws densified enough in order to

solve completely the flows in boundary layers, it should render the flow nature in these zones accurately enough.

3.2 Computational model

The computations were carried out with an ANSYS CFX software package (16.2 version) [11]. To compare the flow characteristics of the radial fan (total compression ratio, power and efficiency) to the results of the experimental investigations, the computations of a steady flow in the fan under consideration were conducted.

The computational model of the fan depicted in Fig. 8 comprised:
- segment of the inlet pipe – fixed domain,
- volute zone from the impeller hub with protruding bolts and nuts fixing movable blades (volute – TT) – rotating domain,
- volute zone from the impeller shroud with protruding bolts and nuts fixing movable blades (volute – TP) – rotating domain,
- impeller composed of an inlet part and a palisade part – rotating domains,
- volute channel – fixed domain.

A 'frozen-rotor' transfer model was applied between the rotating and fixed domains. It consists in recalculation of velocity vector components from the rotating system into the fixed one (or vice versa) for one selected position of movable elements with respect to the fixed ones. The rotational speed of the fan was constant and equaled 1450 rpm.

Air treated as an ideal gas was selected from the CFX database as a fluid. The calculations were made for the reference pressure of 0.1 MPa. The gravitational field effect was neglected. A change in the fluid density and temperature was considered in the equation of state of ideal gas despite a low value of the compression ratio. An SST (shear stress transport) two-equation turbulence model with the wall function was applied.

The following boundary conditions (BC) were taken into account in the computations:
- the velocity profile at the fan inlet pipe (Fig. 8), determined from separate calculations of the inlet channel, in which a simplified straightener and a Venturi pipe were considered. The average value of the axial component was assumed as dependent on the value of the mass flow rate. The circumferential and radial components were equal to 0.0 m/s;
- for the turbulence model, an average value of the turbulence intensity equal to 5% and the value of the turbulent viscosity 10 times higher than the coefficient of air dynamic viscosity were assumed;
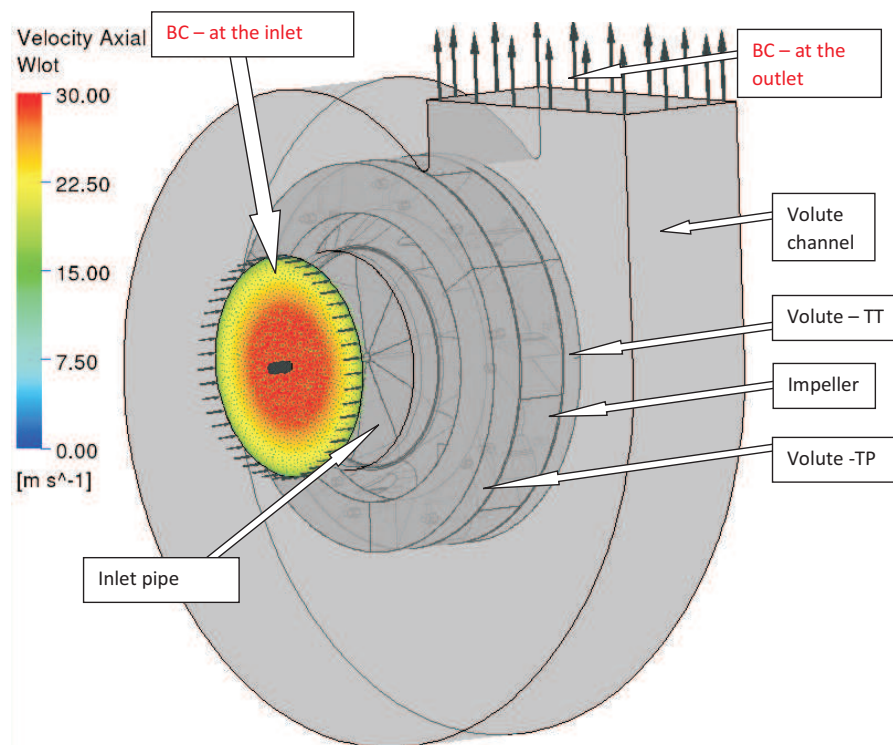- air static temperature at the inlet was equal to 19.6 °C;

Figure 8: Computational domains and location of boundary conditions [9].

- the mean value of the static overpressure at the volume outlet was 0 Pa.
  The nonuniformity coefficient of pressure distribution was assumed to be
  equal to 0.05;
- absolute velocities on fixed element walls in fixed domains and relative ve-
  locities on movable element walls in rotating domains were assumed to be
  zero;
- it was assumed that the circumferential speed resulted from the rotating
  motion on the walls rotating in the fixed domain;
- opposite velocity to the circumferential one was assumed on fixed walls in
  the rotating domain.

The geometrical structure of the fan under analysis is very complex and significant
differences in the results of computations and experimental investigations are sup-
posed to occur in the models with the geometry reproduced in the computational
meshes generated. Simultaneously, the steady state computational method as-

sumed for the unsteady flow will result in rather significant simplifications in flow structures when compared to those that can occur in the real flow. It should also be considered that the calculations were conducted on the assumption of smooth surfaces of fan elements, which in the real flow system can have a considerable effect on the values of individual parameters and their alternations under variable operating conditions of the fan.

The fact that steady flow conditions and the 'frozen-rotor' method, as well as air as an ideal gas were assumed was reflected in the results obtained. It was done intentionally and caused very significant shortening of the computational time.

4   Results

The calculations were conducted with a computational cluster of 8 processors and parallel computing. As a condition to attain the convergence of iterative processes, unbalanced values of momentum rates and mass flow rates on the level of 10^{-4} and stabilization of the monitored quantities such as the total compression ratio and the fanning loss, were assumed. As the second limitation (which resulted from the observations during the computations), the maximal number of iterations equal to 500 was assumed. A high level of obtained residues in the equations of mass and momentum conservation follows from the assumed, partially unsteady nature of the flow (numerous zones of flow separation). Nevertheless, stabilization of values of global parameters that characterize the fan operation proves a satisfactory quality of this solution (Fig. 9).

As a result of the computations, velocity, pressure and stress fields of the fluid were obtained. They were used to determine values of the total compression rate, power and efficiency in every operating point of the fan. These values were calculated with the expressions presented in Tab. 1.

The results of calculations were collected in the form of the relationships between the compression ratio, power, efficiency and the volume flow rate – $\Delta p_c = f(Q)$, $P = f(Q)$, $\eta = f(Q)$ – in comparison to the experimental investigations. Figures 10, 11 and 12 show a comparison of the compression ratio characteristics $\Delta p_c = f(Q)$ for the same positions of the blade tip in its sharp and cut version. The position of the movable blade tip is illustrated on each plot of the compression ratio $\Delta p_c = f(Q)$. A comparison of the computational and experimental characteristics for selected angular positions of the movable part of the impeller blade and its tip versions are plotted in Figs. 13 and 14.
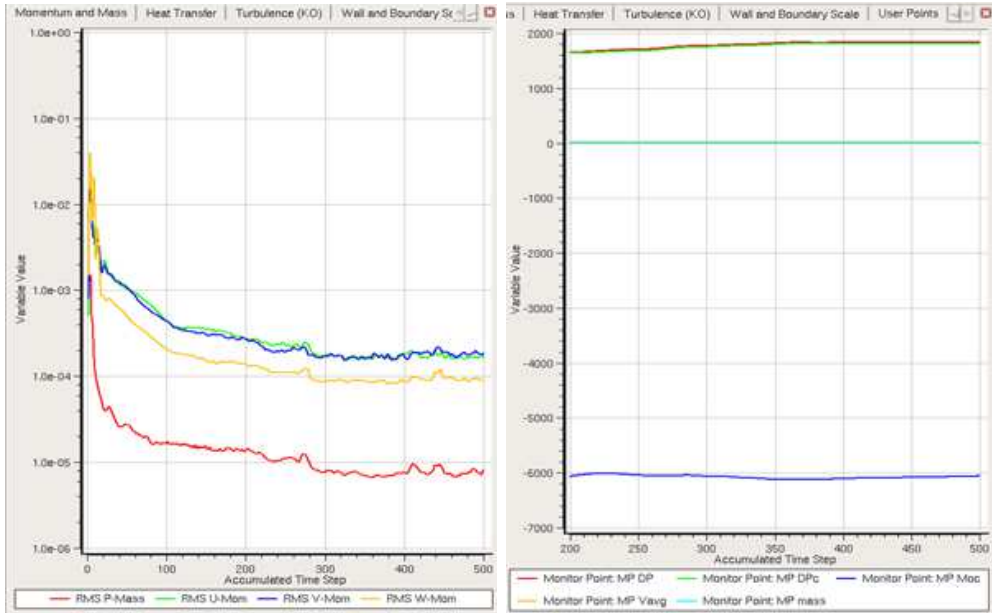
Figure 9: Unbalanced values of mass flow rates and momentum rates (left); values of the compression ratio and power of the fan (right).

Table 1: Parameters of the fan under investigation.

Quantity	Total compression ratio of the fan	Volume flow rate	Transferred power	Loss of power (fanning loss)	Efficiency
Symbol [unit]	Δp_c[Pa]	Q[m^3/s]	P [W]	P_b [W]	η [–]
Formula	$pc_{inlet} - pc_{outlet}$	$\frac{\dot{m}}{\rho}$	$(M_{blade} + M_{hub} + M_{shroud})\,\omega$	$(M_{external\ hub} + M_{external\ shroud})\,\omega$	$\frac{\Delta p_c\,Q}{P+P_b}$
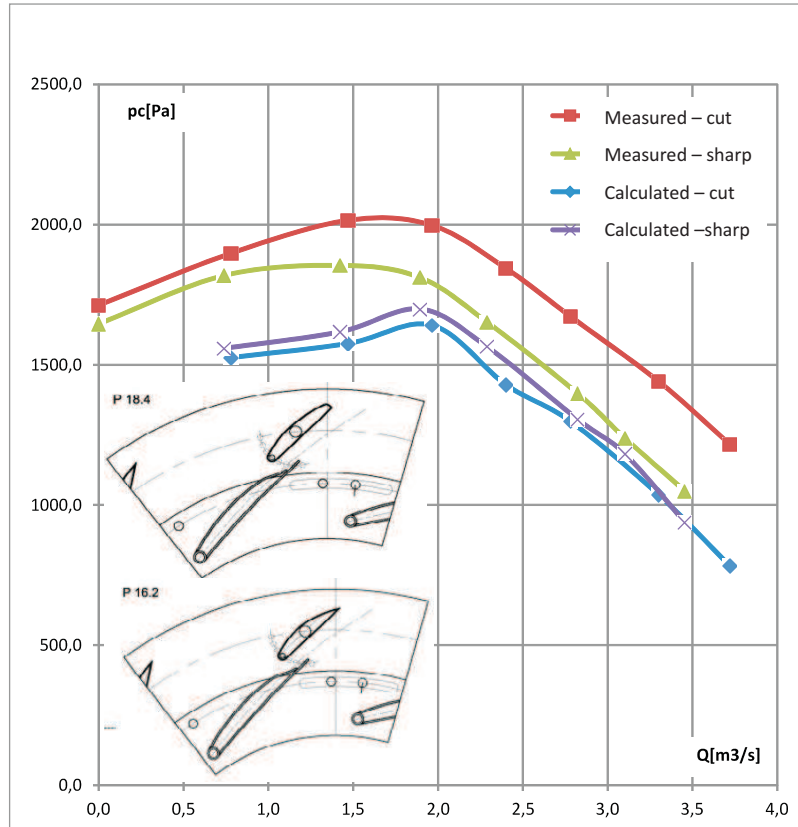
Figure 10: Calculated and determined experimentally compression ratio for the nominal angular position of the blade movable part for the cut and sharp blade tip.

Analysing the obtained results and comparing them to the values determined experimentally, one can state that all the determined characteristics are close to one another as far as their values are concerned only for the maximal deflection angle of the movable part of the blade. The calculated values are shifted towards higher values of the volume flow rate of the medium. For the nominal angle and the minimal angle, the compression ratio of the fan determined on the test stand is higher in the whole range of volume flow rates that the calculated one, and, additionally, it is shifted towards its higher values. For each case, the shape of the flow characteristics is similar. An effect of the blade tip is not explicit, although it can be observed that with a change in the tip angle of the blade movable part from the maximal to the minimal, the sharp tip results in lower

values of the compression ratio. It seems that the above-mentioned assumptions and simplifications and the assumed method of steady calculations decrease an influence of flow turbulences and underestimate fan compression ratios. For the maximal angle, a movable blade part deflection streamlines the flow and thus, the calculated values are close to the experimental ones. In this case, an analysis of flow structures inside stationary and rotating channels will be essential.
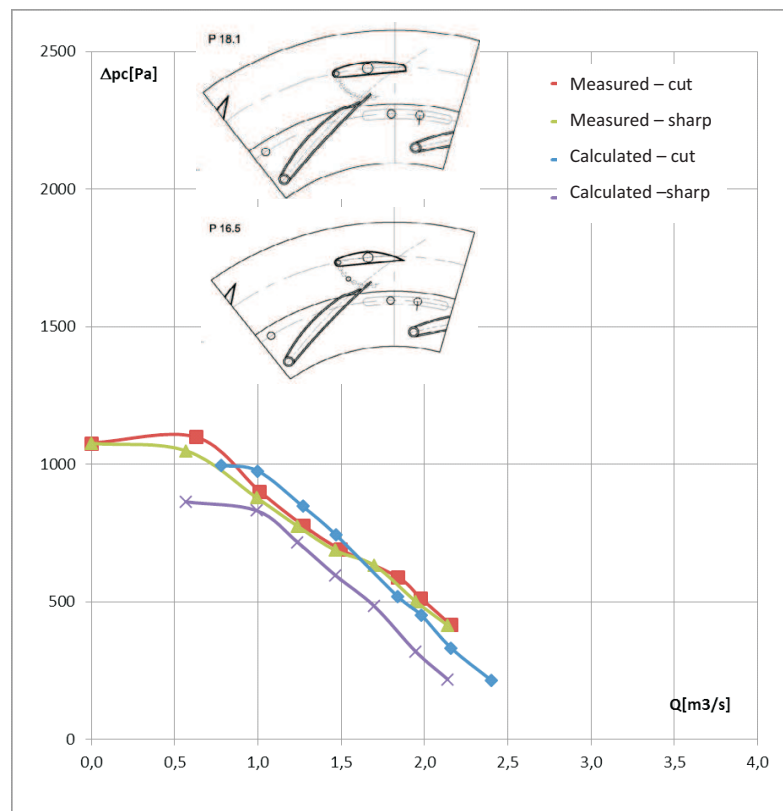

Figure 11: Calculated and determined experimentally compression ratio for the maximum angle of the blade movable part for the cut and sharp blade tip.

Analyzing the obtained values of power and efficiency, one should emphasize the fact that only for the minimal angle of the fan impeller blade movable part, the power calculated and measured are close to each other, and, moreover, the curves cross each other. For the remaining cases, the power determined on the test stand has considerably higher values. As far as efficiency is concerned, the relationships
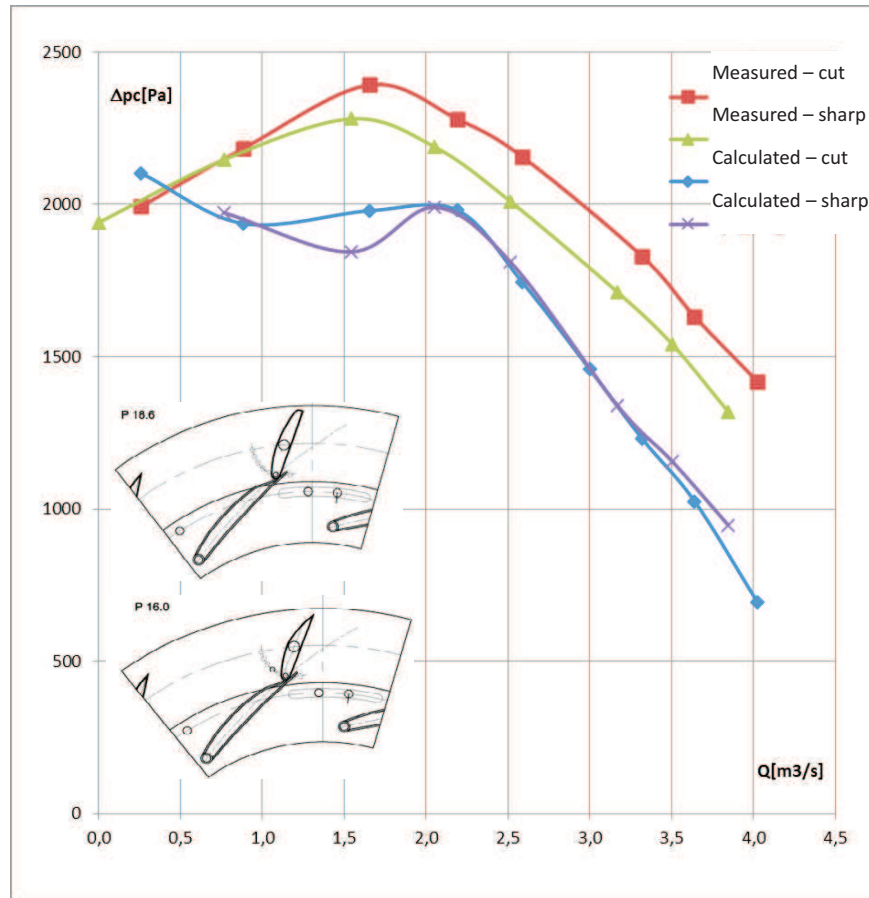
Figure 12: Calculated and determined experimentally compression ratio for the minimal angle of the blade movable part for the cut and sharp blade tip.

are not so explicit. However, the efficiency calculated has a higher value in the middle of the characteristics curve only for the maximal angle.

Table 2 presents values of the force acting on the blade movable part and values of torque necessary to change the blade angular position, calculated on the basis on the determined stress field. On the basis of analysis of the determined values, it can be stated that the torque changes its sign. The structure of the mechanism changing a position of the blade movable part should account for it in order to avoid the phenomenon of flattering.
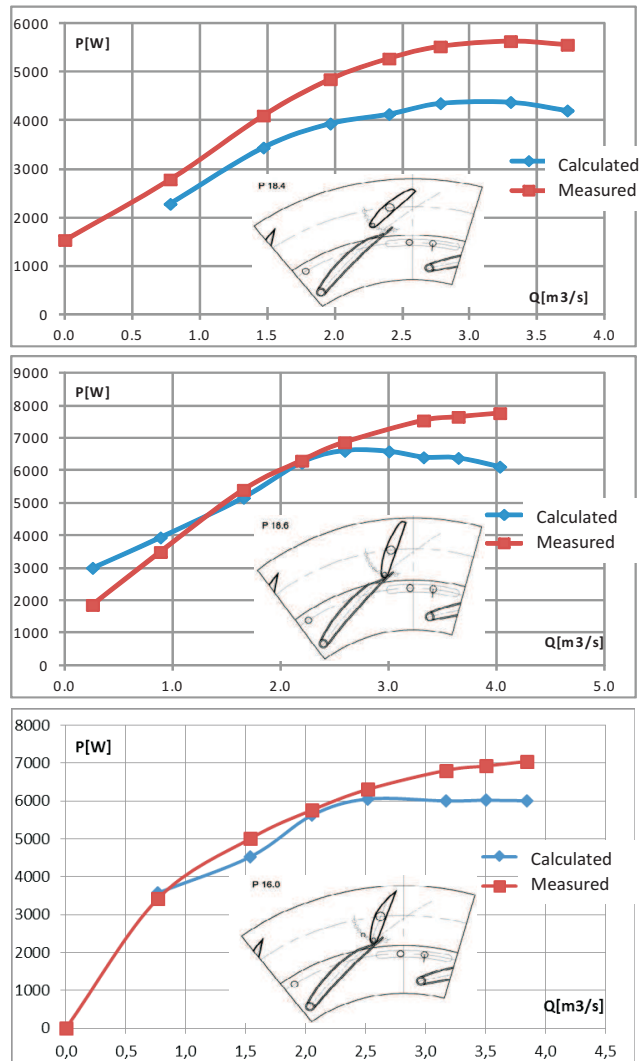
Figure 13: Calculated and determined experimentally fan power for different positions of the blade movable part for the cut and sharp blade tip: upper – nominal angle, cut blade tip; middle – minimal angle, cut blade tip; bottom – minimal angle, sharp blade tip.
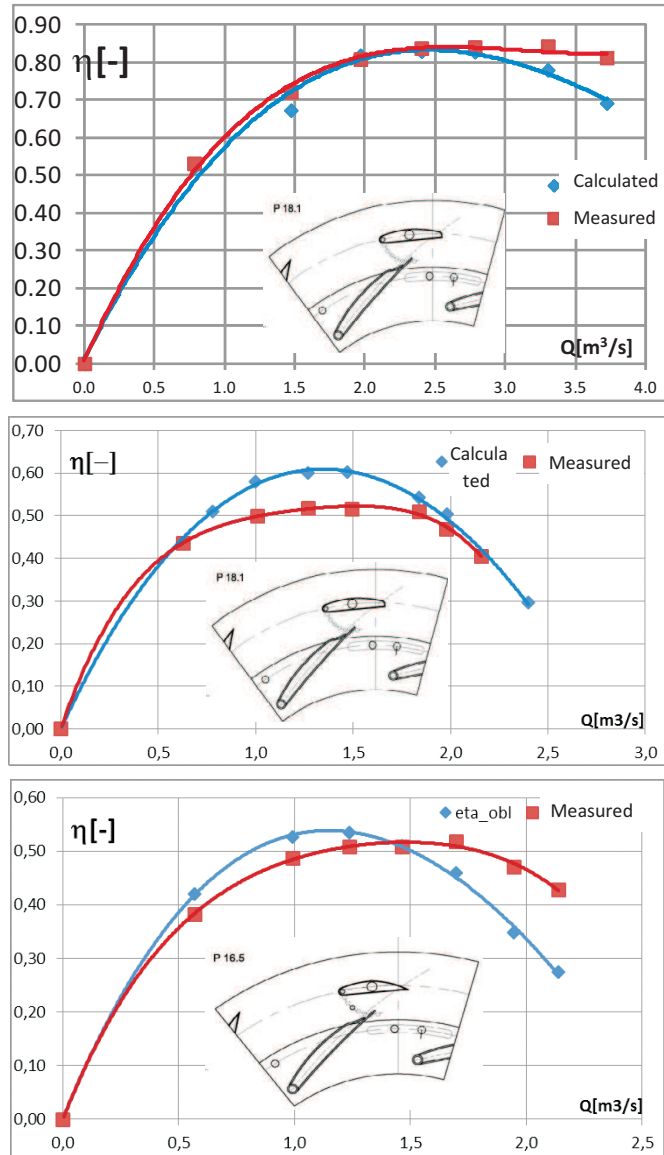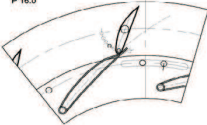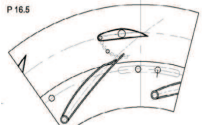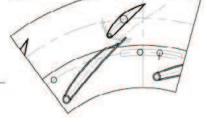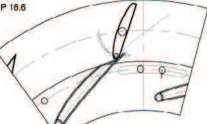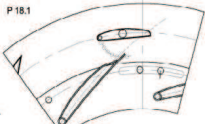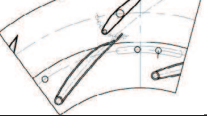
Figure 14: Calculated and determined experimentally fan efficiency for different positions of the blade movable part for the cut and sharp blade tip: upper – nominal angle, cut blade tip; middle – maximal angle, cut blade tip; bottom – maximal angle, sharp blade tip.

Differences between the calculated and measured operating parameters of the fan under investigation are not considerable, but important from the point of view

Table 2: Values of torque and the resultant force acting on the blade which is the closest to a cut-off of the fan volute.

Version and position	Q [m³/s]	M_o [N m]	F [N]
P 16.0	0.765	0.45515	2.48
	1.541	0.02229	3.43
	2.517	0.01196	5.06
	3.847	-0.06000	8.68
P 16.5	0.570	0.12990	6.34
	1.465	0.15801	11.50
	2.139	0.22000	14.92
P 16.2	0.738	-0.9849	4.71
	1.893	-0.06	4.44
	2.824	-0.14125	6,95
	3.455	-0.24	9.46
	Q [m³/s]	M_o [N m]	F [N]
P 16.6	0.256	0.05637	1.02
	1.654	0.04787	6.294
	2.59	-0.00639	5.847
	4.026	-0.14650	9.046
P 18.1	0.78	0.12284	4.135
	1.47	0.16766	7.233
	2.16	0.23325	12.472
P 18.4	0.78	-0.09578	4.66
	2.40	-0.11992	5.34
	3.72	-0.30185	10.087

of the designing process. A matter of some significance is also the way of flow modeling and computational procedures. The assumed method of steady calculations and turbulence modeling entails some inaccuracies and does not account for unsteady phenomena that occur in the flow in full. A view of the phenomena that can be generated, especially when two-part blades of the impeller are used, with one part which is movable and can be adjusted at various angles, is presented in Figs. 15 and 16.
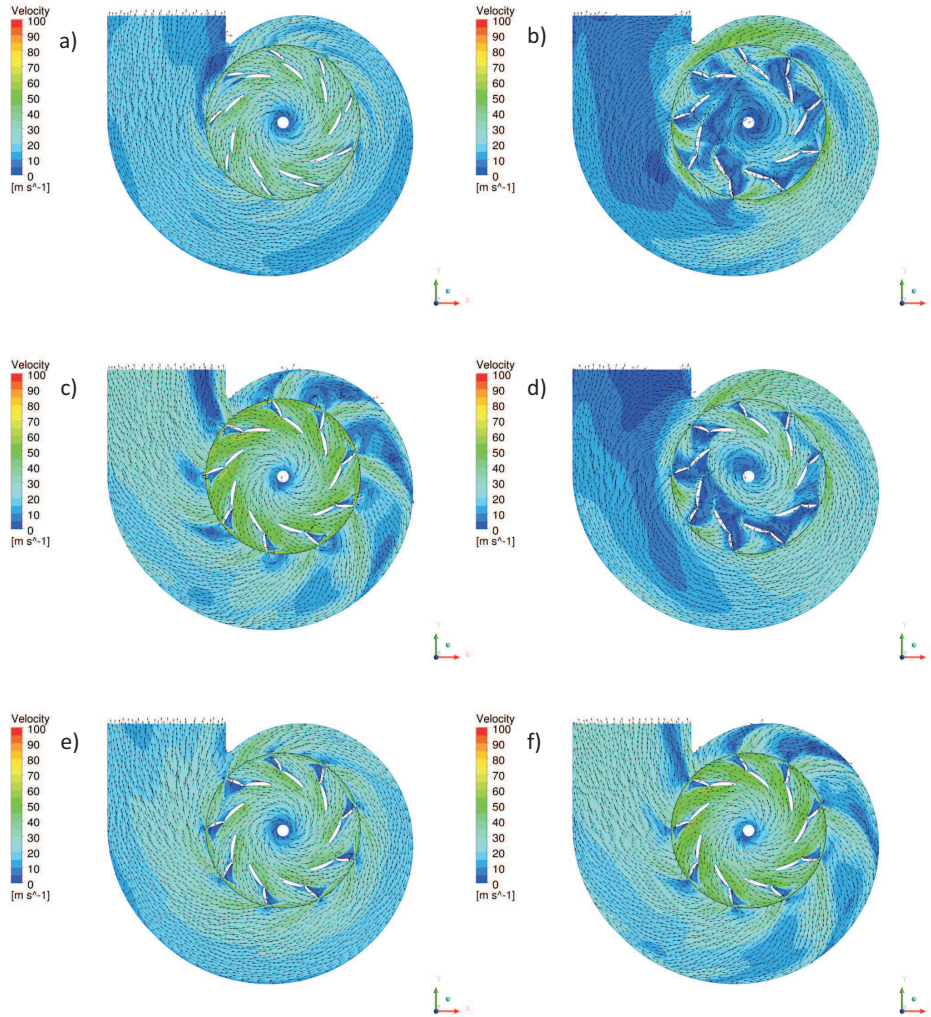
Figure 15: Calculated velocity distribution in the form of a vector field at the average cross-section of the flow path of the investigated fan for selected volume flow rates, different angular positions of blade movable parts and both versions of blade tips: a) cut blade tip, nominal angle, $Q = 2.4$ m^3/s $= Q_n$; b) cut blade tip, minimal angle, $Q = 0.256$ m^3/s $< Q_n$; c) cut blade tip, minimal angle, $Q = 4.026$ m^3/s $> Q_n$; d) sharp blade tip, minimal angle, $Q = 0.765$ m^3/s $< Q_n$; e) sharp blade tip, minimal angle, $Q = 2.517$ m^3/s $= Q_n$; f) sharp blade tip, minimal angle, $Q = 3.847$ m^3/s $> Q_n$ [10].
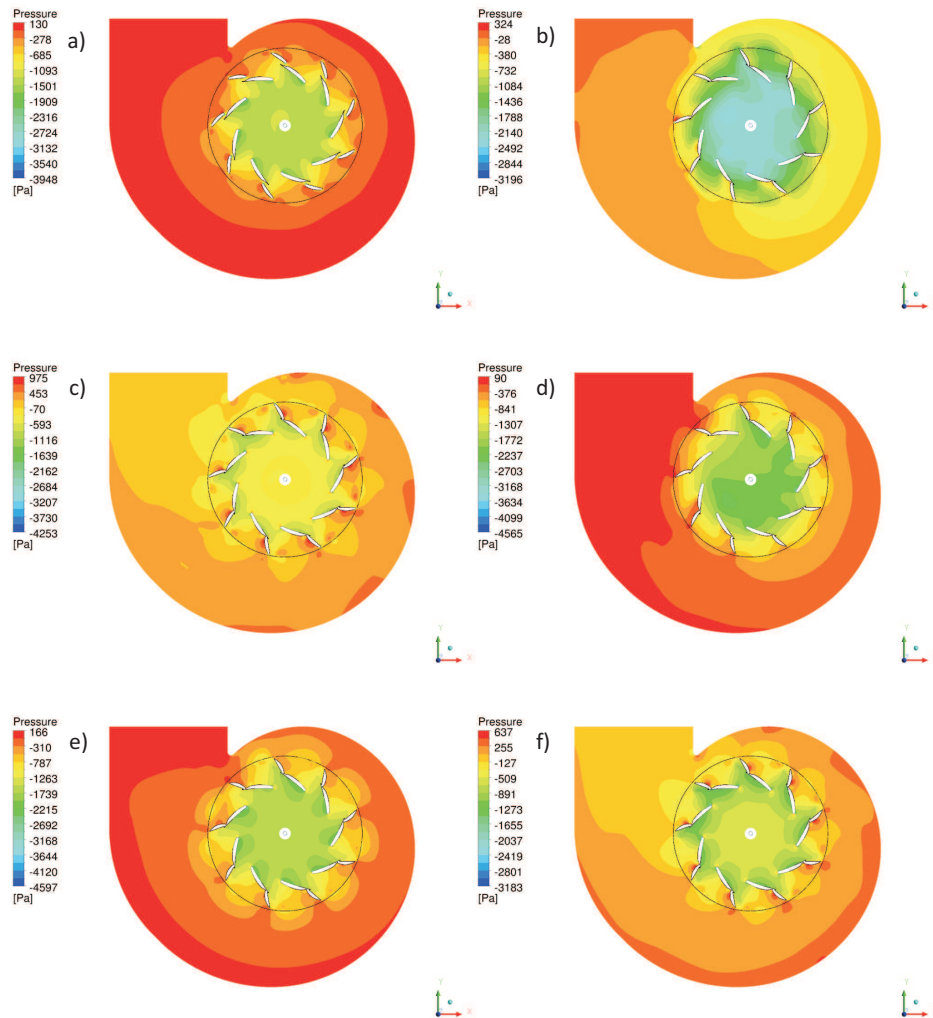
Figure 16: Calculated distribution of static pressure at the average cross-section of the flow path of the investigated fan for selected volume flow rates, different angular positions of blade movable parts and both versions of blade tips: a) cut blade tip, nominal angle, $Q = 2.4 \text{ m}^3/\text{s} = Q_n$; b) cut blade tip, minimal angle, $Q = 0.256 \text{ m}^3/\text{s} < Q_n$; c) cut blade tip, minimal angle, $Q = 4.026 \text{ m}^3/\text{s} > Q_n$; d) sharp blade tip, minimal angle, $Q = 0.765 \text{ m}^3/\text{s} < Q_n$; e) sharp blade tip, minimal angle, $Q = 2.517 \text{ m}^3/\text{s} = Q_n$; f) sharp blade tip, minimal angle, $Q = 3.847 \text{ m}^3/\text{s} > Q_n$ [10].

Despite the assumptions and simplifications involved, one can see zones of high vorticity and flow nonuniformity in the fan impeller blading, in particular for low volume flow rates and the minimal angle of the position of impeller blade movable parts. For higher volume flow rates, higher velocity gradients can be observed, but without swirls.

Figure 15 presents a relative velocity distribution as a vector field at the average impeller cross-section area extended by a velocity field in the volute stationary system for some selected angular positions of movable parts of fan impeller blades and both versions of blade tips. The presented velocity fields indicate high vorticity around movable parts of blades, whose position corresponds to the minimal angle. For the sharp tip of the blade movable part, nonuniformity of the velocity field is higher than for the cut-tipped blade (Fig. 15b,d as well as Fig. 15c,f).

Figure 16 shows a static pressure field at the average cross-section of the impeller and the volute for selected angular positions of movable parts of impeller blades and both versions of blade tips, which correspond to the velocity distributions presented in Fig. 15. For the pressure distributions in the energy transfer system, an effect of the tip geometry of the impeller blade movable part exerts a more considerable influence. Changes in values of static pressure along with an increase in the volume flow rate of the medium discharged by the fan are obvious.

5 Conclusions

The conducted numerical analysis of the flow in the fan under investigation has shown that CFD methods can be a useful design-aiding tool even if steady conditions and simplifications referring to modeling of physical phenomena occurring in the flow, geometry and state of flow channel surfaces are applied. Values of the total compression ratio, $\Delta p_c = f(Q)$, obtained from the calculations are underestimated in the majority of instances. An exception is the case of the cut blade in the maximal angular position, for which the calculated value of the total compression ratio is higher than the experimental one. In all the cases, the fan power was underestimated, despite the fact that the geometry of mounting screws at the external side of the impeller disks was accounted for. It can be explained by the fact that smooth walls were assumed in the calculations, which decreases the value of energy transferred to the medium. The velocity and pressure fields show that for minimal values of efficiency, nonuniformity of operation of impeller individual channels is high and it decreases with an increase in the efficiency. For maximal volume flow rates, an almost uniform velocity field can be observed in individual channels of the impeller. Nonuniformity of the velocity field for low

volume flow rates results from a high pressure gradient along the circumferential direction of the volute. It yields pressure pulsations at the fan volute outlet.

The calculated values of forces and momentums acting on blade movable parts indicate an existence of forces that act along different directions. The mechanism of the fan blade adjustment should take into account a change in the direction of torque to avoid the phenomenon of flattering.

Due to the simultaneous experimental investigations and the numerical analysis, the generation of a neural network employing the data and results obtained from the tests will enable 'matching' the results of the numerical analysis and the values close to the experimental ones and determining an arbitrary point of the performance characteristics of a fan designed in such way. Thus, the CFD analysis is an effective tool to attain characteristic performance parameters of radial fans during the designing process.

Received in July 2016

References

[1] Beczkowski J., Sobczak K., Jóźwik K.: *Model investigations of the radial fan with guide vanes – Part 1 – Experimental investigations.* Turbomachinery **133**(2008), 45–58.

[2] Sobczak K., Beczkowski J., Jóźwik K.: *Model investigations of the radial fan with guide vanes – Part 2 – Numerical investigations.* Turbomachinery **133**(2008), 317–326.

[3] Beczkowski J., Jóźwik K.: *Energy savings of boiler radial fans with new control systems.* Turbomachinery **131**(2007), 99–112 (in Polish).

[4] Beczkowski J., Jóźwik K.: *Modernization of a boiler radial fan without rotor disassembly.* Przegląd Mechaniczny **3**(2011), 11, 41–46 (in Polish).

[5] Fortuna S.: *Investigations of Fans and Compressors.* AGH, Kraków 1999 (in Polish).

[6] Fortuna S.: *Fans. Theoretical Fundamentals, Issues of Design and Maintenance, Applications.* Techwent S.C. Kraków 1999 (in Polish).

[7] Laskowski W., Podsędkowski A., Lewkowicz J. Radwański J.: *Radial fan with adjusted blade tips during rotor motion.* Patent PL52456. Poland, 1967.

[8] Lakowske R., Tischer J.: *Centrifugal fan with variable blade pitch.* Patent US4662819A. USA, 1986.

[9] Jóźwik K. *et al.*: *Numerical calculations of the flow through the investigated models, an analysis of the 1D and 3D theory application range of the CFD method for designing processes of radial fans with a double palisade of blades, as well as investigations of the phenomena occurring in these fans – Part 1.* Internal report of the Institute of Turbomachinery, Lodz University of Technology, Project PBS3/B4/11/2015, 1856 (02, 2016), Lodz (in Polish).

[10] Jóźwik K. *et al.*: *Numerical calculations of the flow through the investigated models, an analysis of the 1D and 3D theory application range of the CFD method for designing processes of radial fans with a double palisade of blades, as well as investigations of the phenomena occurring in these fans – Part 2.* Internal report of the Institute of Turbomachinery, Lodz University of Technology, Project PBS3/B4/11/2015, 1864 (02, 2016), Lodz (in Polish).

[11] ANSYS CFX Theory & Meshing User's Guide. ANSYS Release 16.2 ANSYS Inc.